

J/ψ Inclusive Production in ep Deep-Inelastic Scattering at DESY HERA

BERND A. KNIEHL*

Max-Planck-Institut für Physik (Werner-Heisenberg-Institut),
Föhringer Ring 6, 80805 Munich, Germany

LENNART ZWIRNER

II. Institut für Theoretische Physik, Universität Hamburg,
Luruper Chaussee 149, 22761 Hamburg, Germany

Abstract

We calculate the cross section of J/ψ plus jet associated production in ep deep-inelastic scattering within the factorization formalism of nonrelativistic quantum chromodynamics. Our analytic results disagree with previous analyses, both for the colour-singlet and colour-octet channels. Our theoretical predictions agree reasonably well with recent data taken by the H1 Collaboration at DESY HERA, significantly better than those obtained within the colour-singlet model.

PACS numbers: 12.38.-t, 13.60.Hb, 13.60.Le, 14.40.Gx

*Permanent address: II. Institut für Theoretische Physik, Universität Hamburg, Luruper Chaussee 149, 22761 Hamburg, Germany.

1 Introduction

Since its discovery in 1974, the J/ψ meson has provided a useful laboratory for quantitative tests of quantum chromodynamics (QCD) and, in particular, of the interplay of perturbative and nonperturbative phenomena. The factorization formalism of nonrelativistic QCD (NRQCD) [1] provides a rigorous theoretical framework for the description of heavy-quarkonium production and decay. This formalism implies a separation of short-distance coefficients, which can be calculated perturbatively as expansions in the strong-coupling constant α_s , from long-distance matrix elements (MEs), which must be extracted from experiment. The relative importance of the latter can be estimated by means of velocity scaling rules, i.e. the MEs are predicted to scale with a definite power of the heavy-quark (Q) velocity v in the limit $v \ll 1$. In this way, the theoretical predictions are organized as double expansions in α_s and v . A crucial feature of this formalism is that it takes into account the complete structure of the $Q\bar{Q}$ Fock space, which is spanned by the states $n = {}^{2S+1}L_J^{(c)}$ with definite spin S , orbital angular momentum L , total angular momentum J , and colour multiplicity $c = 1, 8$. In particular, this formalism predicts the existence of colour-octet (CO) processes in nature. This means that $Q\bar{Q}$ pairs are produced at short distances in CO states and subsequently evolve into physical, colour-singlet (CS) quarkonia by the nonperturbative emission of soft gluons. In the limit $v \rightarrow 0$, the traditional CS model (CSM) [2,3] is recovered. The greatest triumph of this formalism was that it was able to correctly describe [4,5] the cross section of inclusive charmonium hadroproduction measured in $p\bar{p}$ collisions at the Fermilab Tevatron [6], which had turned out to be more than one order of magnitude in excess of the theoretical prediction based on the CSM.

In order to convincingly establish the phenomenological significance of the CO processes, it is indispensable to identify them in other kinds of high-energy experiments as well. Studies of charmonium production in ep photoproduction, ep and νN deep-inelastic scattering (DIS), e^+e^- annihilation, $\gamma\gamma$ collisions, and b -hadron decays may be found in the literature; see Ref. [7] and references cited therein. Furthermore, the polarization of charmonium, which also provides a sensitive probe of CO processes, was investigated [8,9,10]. None of these studies was able to prove or disprove the NRQCD factorization hypothesis.

In this paper, we revisit J/ψ inclusive production in ep DIS. In order to avoid kinematic overlap with diffractive production, which cannot yet be reliably described within purely perturbative QCD, we require that the J/ψ meson be produced in association with a hadron jet j , i.e. we consider the process $e + p \rightarrow e + J/\psi + j + X$, where X denotes the proton remnant. In this way, the inelasticity variable z , which measures the fraction of the virtual-photon (γ^*) energy transferred to the J/ψ meson in the proton rest frame, can take values below unity, away from the endpoint $z = 1$, where diffractive production takes place. At the same time, the J/ψ meson can acquire finite transverse momentum p_T^* in the γ^*p centre-of-mass (CM) frame, and the hadronic system X' consisting of the jet j and the proton remnant X can acquire finite mass $M_{X'}$. By the same token, diffractive events can be eliminated from the experimental data sample by applying appropriate acceptance cuts on z , p_T^* , or $M_{X'}$. Another possibility to suppress the diffractive background at $z \lesssim 1$

would be to require that the photon virtuality Q^2 be sufficiently large [11]. However, then also the bulk of the nondiffractive signal would be sacrificed.

The leading CS ME of the J/ψ meson is $\langle \mathcal{O}^\psi [{}^3S_1^{(1)}] \rangle$, its leading CO ones are $\langle \mathcal{O}^\psi [{}^1S_0^{(8)}] \rangle$, $\langle \mathcal{O}^\psi [{}^3S_1^{(8)}] \rangle$, and $\langle \mathcal{O}^\psi [{}^3P_J^{(8)}] \rangle$, with $J = 0, 1, 2$. At LO, we are thus led to consider the partonic subprocesses $e + a \rightarrow e + c\bar{c}[n] + a$, where $a = g, q, \bar{q}$ and $n = {}^3S_1^{(1)}, {}^1S_0^{(8)}, {}^3S_1^{(8)}, {}^3P_J^{(8)}$. Here, q runs over the light-quark flavours u, d , and s . Notice that $e + q(\bar{q}) \rightarrow e + c\bar{c} [{}^3S_1^{(1)}] + q(\bar{q})$ is forbidden because the charm-quark line is connected to one gluon, which transfers colour to the $c\bar{c}$ pair. Representative Feynman diagrams are depicted in Fig. 1. The corresponding cross sections are of $\mathcal{O}(\alpha^2\alpha_s^2)$.

There are several motivations for our study of $e + p \rightarrow e + J/\psi + j + X$ in DIS. For one thing, the H1 Collaboration measured various distributions of this process at DESY HERA [12,13,14], which wait to be confronted with appropriate theoretical predictions. This allows for a particularly clean test of the NRQCD factorization hypothesis, since the large photon virtuality Q^2 ensures that perturbative QCD is applicable and that the resolved-photon contribution, which suffers from our imperfect knowledge of the parton density functions (PDFs) of the photon, is greatly suppressed. Furthermore, at least within the CSM, this process provides a good handle on the gluon PDF of the proton, which is less precisely known than the quark ones. In NRQCD, however, the extraction of the gluon PDF is somewhat aggravated by the presence of the CO channels with a quark or antiquark in the initial state and by the uncertainties associated with the CO MEs. Fortunately, detailed inspection reveals that the relative importance of the quark- and antiquark-induced channels is greatly damped in the HERA regime. We return to this point at the end of Section 3.

On the other hand, in the case of J/ψ inelastic photoproduction, with $Q^2 \approx 0$, NRQCD with CO MEs tuned [5] to fit the Tevatron data [6] predicts [15,16] at leading order (LO) a distinct rise in cross section as $z \rightarrow 1$, which is not observed by the H1 [17] and ZEUS [18] Collaborations at HERA. This CO charmonium anomaly has cast doubts on the validity of the NRQCD factorization hypothesis, which seems so indispensable to interpret the Tevatron data in a meaningful way. Although there are several interesting and promising ideas how to reconcile this data with the NRQCD prediction, e.g. by including dominant higher-order effects [19], by introducing nonperturbative shape functions that resum higher-order corrections related to the kinematics of soft-gluon radiation and to the difference between the partonic and hadronic phase spaces [20], or by endowing the partons inside the proton with intrinsic transverse momentum (k_T) [21], it is of great interest to find out if this anomaly persists, at LO and without resorting to shape functions or k_T effects, if Q^2 is increased to large values.

On the theoretical side, the cross sections of the partonic subprocesses under consideration here constitute an essential ingredient for the calculation of the next-to-leading-order (NLO) corrections to the inclusive cross section of the reaction $e + p \rightarrow e + J/\psi + X$ in DIS, which, at LO, proceeds through the partonic subprocesses $e + g \rightarrow e + c\bar{c}[n]$ with $n = {}^1S_0^{(8)}, {}^3P_J^{(8)}$. The cross sections of the latter are of $\mathcal{O}(\alpha^2\alpha_s)$ and may be found in Eq. (3) of Ref. [22]. In fact, integrating over the phase space of the massless final-state

parton a , one obtains the real radiative corrections. If $a = g$ and $n = {}^1S_0^{(8)}, {}^3P_J^{(8)}$, then they suffer from both infrared (IR) singularities and collinear ones associated with the incoming gluon. The latter are factorized, at some factorization scale M , and absorbed into the bare gluon PDF of the proton, so as to render it renormalized. The IR singularities cancel when the real radiative corrections are combined with the virtual ones. Finally, the ultraviolet (UV) radiative corrections contained in the latter are removed by renormalizing the couplings, masses, wave-functions, and non-perturbative MEs appearing in the LO cross section of $e + p \rightarrow e + J/\psi + X$.

Finally, the literature contains mutually inconsistent formulas for the cross section of the CS partonic subprocess $e + g \rightarrow e + c\bar{c} [{}^3S_1^{(1)}] + g$ [23,24,25,26,27]. On the other hand, there is only one paper specifying analytic results for the cross sections of the CO partonic subprocesses enumerated above [27], so that an independent check seems to be in order. We anticipate that we disagree with all published CS and CO formulas, except with the one referring to $e + g \rightarrow e + c\bar{c} [{}^1S_0^{(8)}] + g$ [27].

This paper is organized as follows. In Section 2, we present, in analytic form, the cross sections of the partonic subprocesses $e + a \rightarrow e + c\bar{c}[n] + a$ enumerated above to LO in NRQCD and explain how to calculate from them the total cross section of $e + p \rightarrow e + J/\psi + j + X$ in DIS and several distributions of phenomenological interest. Lengthy expressions are relegated to the Appendix. In Section 3, we present our numerical results and compare them with recent H1 data [12]. Our conclusions are summarized in Section 4.

2 Analytic results

In this section, we present our analytic results for the cross section of $e + p \rightarrow e + J/\psi + j + X$ in DIS. We work at LO in the parton model of QCD with $n_f = 3$ active quark flavours and employ the NRQCD factorization formalism [1] to describe the formation of the J/ψ meson. We start by defining the kinematics. As indicated in Fig. 2, we denote the four-momenta of the incoming lepton and proton and the outgoing lepton, J/ψ meson, and jet by k , P , k' , p_ψ , and p' , respectively. The parton struck by the virtual photon carries four-momentum $p = xP$. We neglect the masses of the proton, lepton, and light quarks, call the one of the J/ψ meson M_ψ , and take the charm-quark mass to be $m_c = M_\psi/2$. In our approximation, the proton remnant X has zero invariant mass, $M_X^2 = (P - p)^2 = 0$. The CM energy square of the ep collision is $S = (k + P)^2$. The virtual photon has four-momentum $q = k - k'$, and it is customary [28] to define $Q^2 = -q^2 > 0$ and $y = q \cdot P / k \cdot P$, which measures the relative lepton energy loss in the proton rest frame. The inelasticity variable, which was already mentioned in the Introduction, is defined as $z = p_\psi \cdot P / q \cdot P$. The system X' consisting of the jet j and the proton remnant X has invariant mass square $M_{X'}^2 = (q + P - p_\psi)^2 = (1 - x)y(1 - z)S$. Other frequently employed variables [28] are Bjorken's variable $x_B = Q^2 / (2q \cdot P) = Q^2 / (yS)$ and the γ^*p CM energy square $W^2 = (q + P)^2 = yS - Q^2$. As usual, we define the partonic Mandelstam variables as $\hat{s} = (q + p)^2 = xyS - Q^2$, $\hat{t} = (q - p_\psi)^2 = -xy(1 - z)S$, and $\hat{u} = (p - p_\psi)^2 = M_\psi^2 - xyzS$.

By four-momentum conservation, we have $\hat{s} + \hat{t} + \hat{u} = M_\psi^2 - Q^2$. In the γ^*p CM frame, the J/ψ meson has transverse momentum and rapidity

$$p_T^* = \frac{\sqrt{\hat{t}(\hat{s}\hat{u} + Q^2 M_\psi^2)}}{\hat{s} + Q^2}, \quad (1)$$

$$y_\psi^* = \frac{1}{2} \ln \frac{\hat{s}(M_\psi^2 - \hat{u})}{\hat{s}(M_\psi^2 - \hat{t}) + Q^2 M_\psi^2} + \frac{1}{2} \ln \frac{W^2}{\hat{s}}, \quad (2)$$

respectively. Here and in the following, we denote the quantities referring to the γ^*p CM frame by an asterisk. The second term on the right-hand side of Eq. (2) originates from the Lorentz boost from the γ^*a CM frame to the γ^*p one. Here, y_ψ^* is taken to be positive in the direction of the three-momentum of the virtual photon, in accordance with the convention of Refs. [12,13,14].

In the parton model, the proton is characterized by its PDFs $f_{a/p}(x, M)$, and, at LO, an outgoing parton may be identified with a jet. Thus, we have

$$d\sigma(e + p \rightarrow e + J/\psi + j + X) = \int_0^1 dx \sum_a f_{a/p}(x, M) d\sigma(e + a \rightarrow e + J/\psi + a), \quad (3)$$

where $a = g, u, \bar{u}, d, \bar{d}, s, \bar{s}$. Furthermore, according to the NRQCD factorization formalism, we have

$$d\sigma(e + a \rightarrow e + J/\psi + a) = \sum_n \langle \mathcal{O}^\psi[n] \rangle d\sigma(e + a \rightarrow e + c\bar{c}[n] + a), \quad (4)$$

where, to LO in v , $n = {}^3S_1^{(1)}, {}^1S_0^{(8)}, {}^3S_1^{(8)}, {}^3P_J^{(8)}$.

Decomposing the transition-matrix element of the partonic subprocess $e + a \rightarrow e + c\bar{c}[n] + a$ into a leptonic part, $\mathcal{T}^\mu(e \rightarrow e + \gamma^*) = -(e/q^2)\bar{u}(k')\gamma^\mu u(k)$, and a hadronic one, $\mathcal{T}^\mu(\gamma^* + a \rightarrow c\bar{c}[n] + a)$, from which the virtual-photon leg is amputated, we can write its cross section as

$$d\sigma(e + a \rightarrow e + c\bar{c}[n] + a) = \frac{1}{2xS} \frac{1}{4N_a} \frac{e^2}{(q^2)^2} \text{tr}(\not{k}\gamma^\nu \not{k}'\gamma^\mu) H_{\mu\nu} d\text{PS}_3(k + p; k', p_\psi, p'), \quad (5)$$

where $N_g = (N_c^2 - 1)$ and $N_q = N_{\bar{q}} = N_c = 3$ are the colour multiplicities of the partons a , e is the electron charge magnitude, and the hadronic tensor $H^{\mu\nu}$ is obtained by summing the absolute square of $\mathcal{T}^\mu(\gamma^* + a \rightarrow c\bar{c}[n] + a)$ over the spin and colour states of the incoming and outgoing partons a . Here and in the following, we employ the Lorentz-invariant phase-space measure

$$d\text{PS}_n(p; p_1, \dots, p_n) = (2\pi)^4 \delta^{(4)}\left(p - \sum_{i=1}^n p_i\right) \prod_{i=1}^n \frac{d^3 p_i}{(2\pi)^3 2p_i^0}. \quad (6)$$

The first factor in Eq. (5) stems from the flux and the second one from the average over the spin and colour states of the incoming particles. Integrating over the azimuthal angle

of the outgoing lepton, we may simplify Eq. (5) to become

$$d\sigma(e + a \rightarrow e + c\bar{c}[n] + a) = \frac{1}{2xS} \frac{1}{4N_a} \frac{\alpha}{2\pi} L^{\mu\nu} H_{\mu\nu} \frac{dy}{y} \frac{dQ^2}{Q^2} d\text{PS}_2(q + p; p_\psi, p'), \quad (7)$$

where $\alpha = e^2/(4\pi)$ is Sommerfeld's fine-structure constant and [29]

$$L^{\mu\nu} = \frac{1 + (1 - y)^2}{y} \epsilon_T^{\mu\nu} - \frac{4(1 - y)}{y} \epsilon_L^{\mu\nu}, \quad (8)$$

with

$$\begin{aligned} \epsilon_T^{\mu\nu} &= -g^{\mu\nu} + \frac{1}{q \cdot p} (q^\mu p^\nu + p^\mu q^\nu) - \frac{q^2}{(q \cdot p)^2} p^\mu p^\nu, \\ \epsilon_L^{\mu\nu} &= \frac{1}{q^2} \left(q - \frac{q^2}{q \cdot p} p \right)^\mu \left(q - \frac{q^2}{q \cdot p} p \right)^\nu, \end{aligned} \quad (9)$$

is the leptonic tensor. We have $q_\mu \epsilon_T^{\mu\nu} = q_\mu \epsilon_L^{\mu\nu} = 0$, $\epsilon_{T\mu}^\mu = -2$, and $\epsilon_{L\mu}^\mu = -1$. Furthermore,

$$\epsilon^{\mu\nu} = \epsilon_T^{\mu\nu} + \epsilon_L^{\mu\nu} = -g^{\mu\nu} + \frac{q^\mu q^\nu}{q^2} \quad (10)$$

is the polarization tensor of an unpolarized spin-one boson with mass q^2 . In the γ^*a CM frame, where $q^\mu = (q^0, 0, 0, q^3)$ and $p^\mu = (q^3, 0, 0, -q^3)$, we have $\epsilon_T^{\mu\nu} = \text{diag}(0, 1, 1, 0)$ and $\epsilon_L^{\mu\nu} = (1/q^2)(q^3, 0, 0, q^0)^\mu (q^3, 0, 0, q^0)^\nu$, so that $\epsilon_T^{\mu\nu}$ and $\epsilon_L^{\mu\nu}$ refer to transverse and longitudinal polarization, as indicated by their subscripts. Since the hadronic current is conserved in QED, we have $q_\mu H^{\mu\nu} = 0$, which leads to a further simplification as Eq. (8) is inserted in Eq. (7).

It is interesting to study the photoproduction limit, by taking $Q^2 \rightarrow 0$ in Eq. (7). This provides us with a powerful check for our results by relating them to well-known results in the literature [2,9,16]. The differential cross section of the partonic process $\gamma + a \rightarrow c\bar{c}[n] + a$ reads

$$d\sigma(\gamma + a \rightarrow c\bar{c}[n] + a) = \frac{1}{2\hat{s}} \frac{1}{4N_a} (-g^{\mu\nu}) H_{\mu\nu}|_{Q^2=0} d\text{PS}_2(q + p; p_\psi, p'). \quad (11)$$

Comparing Eqs. (7) and (11), we thus obtain the master formula

$$\lim_{Q^2 \rightarrow 0} \frac{Q^2 d^2\sigma}{dy dQ^2} (e + a \rightarrow e + c\bar{c}[n] + a) = \frac{\alpha}{2\pi} \frac{1 + (1 - y)^2}{y} \sigma(\gamma + a \rightarrow c\bar{c}[n] + a). \quad (12)$$

A similar relationship between the DIS process $e + p \rightarrow e + J/\psi + X$ and the photoproduction one $\gamma + p \rightarrow J/\psi + X$ may be found in Eq. (4) of Ref. [22].

We evaluate the cross sections of the relevant partonic subprocesses $e + a \rightarrow e + c\bar{c}[n] + a$ from Eq. (7) applying the covariant-projector method of Ref. [30]. Our results can be written in the form

$$\frac{d^3\sigma}{dy dQ^2 d\hat{t}} (e + a \rightarrow e + c\bar{c}[n] + a) = \frac{\alpha}{2\pi} F_a[n] \left[\frac{1 + (1 - y)^2}{yQ^2} T_a[n] - \frac{4(1 - y)}{y} L_a[n] \right], \quad (13)$$

where $F_a[n]$, $T_a[n]$, and $L_a[n]$ are functions of \hat{s} , \hat{t} , \hat{u} , and Q^2 , which are listed in the Appendix. They are finite for $Q^2 = 0$. We combined the results for $n = {}^3P_J^{(8)}$, with $J = 0, 1, 2$, exploiting the multiplicity relation

$$\langle \mathcal{O}^\psi [{}^3P_J^{(8)}] \rangle = (2J + 1) \langle \mathcal{O}^\psi [{}^3P_0^{(8)}] \rangle, \quad (14)$$

which follows to LO in v from heavy-quark spin symmetry. We recover the well-known cross sections of the corresponding CS [2] and CO [9,16] processes of photoproduction by inserting Eq. (13) in Eq. (12), as

$$\frac{d\sigma}{dt}(\gamma + a \rightarrow c\bar{c}[n] + a) = F_a[n]T_a[n]|_{Q^2=0}. \quad (15)$$

At this point, we should compare our analytic results with the literature. Formulas for the cross section of the CS partonic subprocess $e + g \rightarrow e + c\bar{c} [{}^3S_1^{(1)}] + g$ may be found in Refs. [23,24,25,26,27]. In Ref. [27], also cross section formulas for the CO partonic subprocesses $e + a \rightarrow e + c\bar{c}[n] + a$ with $a = g, q, \bar{q}$ and $n = {}^1S_0^{(8)}, {}^3S_1^{(8)}, {}^3P_J^{(8)}$ are listed. We agree with the result for $e + g \rightarrow e + c\bar{c} [{}^1S_0^{(8)}] + g$ [27], but we disagree with all the other results. In particular, the results of Refs. [23,25] and the residual results of Ref. [27] fail to reproduce the well-established formulas of Refs. [2,9,16] in the photoproduction limit. We also remark that Eqs. (A21) and (A35)–(A37) of Ref. [27] suffer from mass-dimensional inconsistencies. Furthermore, we only find agreement with the result in Eq. (4) of Ref. [24] if we flip the overall sign of $L_a[n]$ in Eq. (13). However, this causes the cross section in Eq. (13) to turn negative in certain regions of phase space, e.g. at $y = 0.5$, $Q^2 = 25 \text{ GeV}^2$, $\hat{s} = 100 \text{ GeV}^2$, and $\hat{t} = -10 \text{ GeV}^2$. Similarly, we only agree with the result in Eq. (2.49) of Ref. [26] if we include an overall factor of $4\pi\alpha$ on the right-hand side of Eq. (13) and halve $L_a[n]$. As for the cross sections of the CO partonic subprocesses $e + g \rightarrow e + c\bar{c}[n]$ with $n = {}^1S_0^{(8)}, {}^3P_J^{(8)}$, which do not enter our analysis, we agree with Eq. (3) of Ref. [22].

The cross sections of $e + g \rightarrow e + c\bar{c}[n] + g$ with $n = {}^1S_0^{(8)}, {}^3P_J^{(8)}$ exhibit collinear singularities in the limit $\hat{t} \rightarrow 0$. According to the factorization theorem of the QCD-improved parton model, the limiting expressions must coincide with the $e + g \rightarrow e + c\bar{c}[n]$ cross sections [22] multiplied by the spacelike $g \rightarrow g$ splitting functions. This provides another nontrivial check for our results, and, among other things, this fixes the overall factor of $L_a[n]$.

Inserting Eq. (4) in Eq. (3) and including the maximum boundaries of the integrations over x and \hat{t} , we obtain

$$\begin{aligned} \frac{d^2\sigma}{dy dQ^2}(e + p \rightarrow e + J/\psi + j + X) &= \int_{(Q^2+M_\psi^2)/(yS)}^1 dx \int_{-(\hat{s}+Q^2)(\hat{s}-M_\psi^2)/\hat{s}}^0 d\hat{t} \\ &\times \sum_a f_{a/p}(x, M) \sum_n \langle \mathcal{O}^\psi[n] \rangle \frac{d^3\sigma}{dy dQ^2 d\hat{t}}(e + a \rightarrow e + c\bar{c}[n] + a), \end{aligned} \quad (16)$$

where $(d^3\sigma/dy dQ^2 d\hat{t})(e + a \rightarrow e + c\bar{c}[n] + a)$ is given by Eq. (13). The kinematically allowed ranges of y and Q^2 are $M_\psi^2/S < y < 1$ and $0 < Q^2 < yS - M_\psi^2$, respectively. In

order to avoid the collinear singularities mentioned above, we need to reduce the upper boundary of the \hat{t} integration in Eq. (16). This cut-off should, of course, depend on variables that can be controlled experimentally. It is convenient to introduce an upper cut-off, below unity, on the inelasticity variable z . As explained in the Introduction, such a cut-off also suppresses the diffractive background. The distributions in y and Q^2 can be evaluated from Eq. (16) as it stands. It is also straightforward to obtain the distributions in z , x_B , W , p_T^* , and y_ψ^* , by accordingly redefining and reordering the integration variables in Eq. (16). The distribution in the J/ψ azimuthal angle ϕ^* in the γ^*p CM frame is constant.

The evaluation of the distributions in the J/ψ transverse momentum p_T , rapidity y_ψ , and azimuthal angle ϕ in the HERA laboratory frame is somewhat more involved. Choosing a suitable coordinate system in the γ^*p CM frame, we have

$$\begin{aligned}
(k^*)^\mu &= \frac{S - Q^2}{2W} \begin{pmatrix} 1 \\ \sin \psi^* \\ 0 \\ \cos \psi^* \end{pmatrix}, & (k'^*)^\mu &= \frac{S - W^2}{2W} \begin{pmatrix} 1 \\ \sin \theta^* \\ 0 \\ \cos \theta^* \end{pmatrix}, \\
(q^*)^\mu &= \frac{1}{2W} \begin{pmatrix} W^2 - Q^2 \\ 0 \\ 0 \\ W^2 + Q^2 \end{pmatrix}, & (P^*)^\mu &= \frac{W^2 + Q^2}{2W} \begin{pmatrix} 1 \\ 0 \\ 0 \\ -1 \end{pmatrix}, \\
(p_\psi^*)^\mu &= \begin{pmatrix} m_T^* \cosh y_\psi^* \\ p_T^* \cos \phi^* \\ p_T^* \sin \phi^* \\ m_T^* \sinh y_\psi^* \end{pmatrix},
\end{aligned} \tag{17}$$

where $\cos \psi^* = 2SW^2/[(S - Q^2)(W^2 + Q^2)] - 1$, $\cos \theta^* = 1 - 2SQ^2/[(S - W^2)(W^2 + Q^2)]$, and $m_T^* = \sqrt{M_\psi^2 + (p_T^*)^2}$ is the J/ψ transverse mass. On the other hand, in the laboratory frame, we have

$$\begin{aligned}
k^\mu &= E_e \begin{pmatrix} 1 \\ 0 \\ 0 \\ 1 \end{pmatrix}, & (k')^\mu &= E'_e \begin{pmatrix} 1 \\ \sin \theta \\ 0 \\ \cos \theta \end{pmatrix}, \\
q^\mu &= \begin{pmatrix} q^0 \\ -q \sin \psi \\ 0 \\ q \cos \psi \end{pmatrix}, & P^\mu &= E_p \begin{pmatrix} 1 \\ 0 \\ 0 \\ -1 \end{pmatrix}, \\
p_\psi^\mu &= \begin{pmatrix} m_T \cosh y_\psi \\ p_T \cos \phi \\ p_T \sin \phi \\ m_T \sinh y_\psi \end{pmatrix},
\end{aligned} \tag{18}$$

where E_e and E_p are the lepton and proton energies, respectively, $E'_e = [(S - W^2 - Q^2)/E_p + Q^2/E_e]/4$, $\cos \theta = 1 - Q^2/(2E_e E'_e)$, $q^0 = [(W^2 + Q^2)/E_p - Q^2/E_e]/4$, $q = \sqrt{Q^2 + (q^0)^2}$, $\cos \psi = [(W^2 + Q^2)/E_p + Q^2/E_e]/(4q)$, and $m_T = \sqrt{M_\psi^2 + p_T^2}$ is the J/ψ transverse mass. Notice that y_ψ is taken to be positive in the direction of the three-momentum of the incoming lepton. Without loss of generality, we may require that $0 \leq \psi^*, \psi \leq \pi$, for, otherwise, we can achieve this by rotating the respective coordinate systems by 180° around the z axis. We can then evaluate p_T , y_ψ , and ϕ from p_T^* , y_ψ^* , and ϕ^* as

$$p_T = \sqrt{(p_T^*)^2 + A(A - 2p_T^* \cos \phi^*)}, \quad (19)$$

$$y_\psi = y_\psi^* + \ln \frac{(W^2 + Q^2)m_T^*}{\sqrt{S}Wm_T} + \frac{1}{2} \ln \frac{E_e}{E_p}, \quad (20)$$

$$\cos \phi = \frac{p_T^* \cos \phi^* - A}{p_T}, \quad (21)$$

where

$$A = \frac{m_T^* \exp(y_\psi^*) \sin \psi^*}{1 + \cos \psi^*} = \sqrt{\frac{Q^2(S - W^2 - Q^2)}{SW^2}} m_T^* \exp(y_\psi^*). \quad (22)$$

The third term on the right-hand side of Eq. (20) stems from the Lorentz boost from the ep CM frame to the laboratory one. Since p_T , y_ψ , and ϕ depend on ϕ^* , the integration over ϕ^* in Eq. (16) is no longer trivial, and we need to insert the symbolic factor $(1/2\pi) \int_0^{2\pi} d\phi^*$ on the right-hand side of that equation.

For future applications, we also present compact formulas that allow us to determine p_T^* , y_ψ^* , and ϕ^* , once p_T , y_ψ , and ϕ are given. In fact, Eqs. (19) and (21) can be straightforwardly inverted by observing that the quantity A defined in Eq. (22) can be expressed in terms of m_T and y_ψ by substituting Eq. (20), the result being

$$A = \frac{m_T \exp(y_\psi)}{W^2 + Q^2} \sqrt{\frac{E_p}{E_e} Q^2 (S - W^2 - Q^2)}. \quad (23)$$

Having obtained p_T^* , we can then evaluate y_ψ^* from Eq. (20). For the reader's convenience, we collect the relevant formulas here:

$$\begin{aligned} p_T^* &= \sqrt{p_T^2 + A(A + 2p_T \cos \phi)}, \\ y_\psi^* &= y_\psi + \ln \frac{\sqrt{S}Wm_T}{(W^2 + Q^2)m_T^*} + \frac{1}{2} \ln \frac{E_p}{E_e}, \\ \cos \phi^* &= \frac{p_T \cos \phi + A}{p_T^*}. \end{aligned} \quad (24)$$

3 Numerical results

We are now in a position to present our numerical results. We first describe our theoretical input and the kinematic conditions. We use $m_c = (1.5 \pm 0.1)$ GeV, $\alpha = 1/137.036$, and

the LO formula for $\alpha_s^{(n_f)}(\mu)$ with $n_f = 3$ active quark flavours [28]. As for the proton PDFs, we employ the LO set by Martin, Roberts, Stirling, and Thorne (MRST98LO) [31], with asymptotic scale parameter $\Lambda^{(4)} = 174$ MeV, as our default and the LO set by the CTEQ Collaboration (CTEQ5L) [32], with $\Lambda^{(4)} = 192$ MeV, for comparison. The corresponding values of $\Lambda^{(3)}$ are 204 MeV and 224 MeV, respectively. We choose the renormalization and factorization scales to be $\mu = M = \xi \sqrt{Q^2 + M_\psi^2}$ and vary the scale parameter ξ between 1/2 and 2 around the default value 1. We adopt the NRQCD MEs from Table I of Ref. [10]. Specifically, they read $\langle \mathcal{O}^\psi [{}^3S_1^{(1)}] \rangle = (1.3 \pm 0.1) \text{ GeV}^3$, $\langle \mathcal{O}^\psi [{}^3S_1^{(8)}] \rangle = (4.4 \pm 0.7) \times 10^{-3} \text{ GeV}^3$, and $M_{3,4}^\psi = (8.7 \pm 0.9) \times 10^{-2} \text{ GeV}^3$ for set MRST98LO, where

$$M_r^\psi = \langle \mathcal{O}^\psi ({}^1S_0^{(8)}) \rangle + \frac{r}{m_c^2} \langle \mathcal{O}^\psi ({}^3P_0^{(8)}) \rangle. \quad (25)$$

The corresponding values for set CTEQ5L are $(1.4 \pm 0.1) \text{ GeV}^3$, $(3.9 \pm 0.7) \times 10^{-3} \text{ GeV}^3$, and $(6.6 \pm 0.7) \times 10^{-2} \text{ GeV}^3$, respectively. Since Eq. (16) is sensitive to a different linear combination of $\langle \mathcal{O}^\psi ({}^1S_0^{(8)}) \rangle$ and $\langle \mathcal{O}^\psi ({}^3P_0^{(8)}) \rangle$ than appears in Eq. (25), we write $\langle \mathcal{O}^\psi ({}^1S_0^{(8)}) \rangle = \kappa M_r^\psi$ and $\langle \mathcal{O}^\psi ({}^3P_0^{(8)}) \rangle = (1 - \kappa) (m_c^2/r) M_r^\psi$ and vary κ between 0 and 1 around the default value 1/2. In order to estimate the theoretical uncertainties in our predictions, we vary the unphysical parameters ξ and κ as indicated above, take into account the experimental errors on m_c and the default MEs, and switch from our default PDF set to the CTEQ5L one, properly adjusting $\Lambda^{(3)}$ and the MEs. We then combine the individual shifts in quadrature.

The H1 data on J/ψ inclusive and inelastic production in DIS [12,13] were taken in collisions of positrons with $E_e = 27.5 \text{ GeV}$ and protons with $E_p = 820 \text{ GeV}$ in the HERA laboratory frame, so that $\sqrt{S} = 2\sqrt{E_e E_p} = 300 \text{ GeV}$, and they refer to the kinematic region defined by $2 < Q^2 < 80 \text{ GeV}^2$, $40 < W < 180 \text{ GeV}$, and $z > 0.2$. In Ref. [13], the acceptance cut $M_{X'} > 10 \text{ GeV}$ on the invariant mass of the hadronic system X' produced in association with the J/ψ meson was imposed in order to exclude the contribution of J/ψ elastic production, which, to a large extent, is due to diffractive processes. Notice that this cut allows for z to be as large as $z_{\max} = 1 - M_{X',\min}^2 / (W_{\max}^2 - M_\psi^2) \approx 0.997$ and for $|\hat{t}|$ to be as small as $|\hat{t}|_{\min} = (1 - z_{\max}) (Q_{\min} + M_\psi^2) \approx 0.040 \text{ GeV}^2$. A more conservative way to eliminate the domain of J/ψ elastic production is to directly impose the cut $z < 0.9$ [12], which ensures that $|\hat{t}|$ is in excess of $|\hat{t}|_{\min} \approx 1.3 \text{ GeV}^2$. At the same time, a sufficiently large lower bound on $|\hat{t}|$ is requisite in order to screen Eq. (16) from the collinear singularities in the ${}^1S_0^{(8)}$ and ${}^3P_J^{(8)}$ channels, mentioned in Section 2, and, thus, to keep our theoretical predictions perturbatively stable. In the following, we, therefore, use the H1 data with the cut $z < 0.9$, as presented in Ref. [12], for comparisons.

In Figs. 3–7, we confront the measured Q^2 , p_T^2 , z , y^* , and W distributions, respectively, with our NRQCD predictions. For comparison, we also show the corresponding CSM predictions. In each case, the theoretical errors, evaluated as explained above, are indicated by the hatched areas. Instead of presenting our theoretical predictions as con-

tinuous curves, we adopt the binning pattern encoded in the experimental data, so as to facilitate quantitative comparisons. As for the Q^2 and p_T^2 distributions, the experimental data agrees rather well with the NRQCD predictions, both in normalization and shape, while it significantly overshoots the CSM predictions. In the case of the z distribution, the NRQCD prediction, in general, agrees better with the experimental data than the CSM one as far as the normalization is concerned. As for the shape, however, the experimental measurement favours the CSM prediction, while the NRQCD one exhibits an excess at large values of z , which is familiar from J/ψ inclusive photoproduction [15,16]. As in the latter case, this rise in z is chiefly due to the $^1S_0^{(8)}$ and $^3P_J^{(8)}$ channels. In the case of the y^* distribution, the NRQCD prediction nicely agrees with the experimental data for $y^* < 3$, while it appreciably overshoots the latter in the very forward direction. The CSM prediction roughly agrees with the experimental y^* distribution at the endpoints, while it significantly falls short of the latter in the central region. In the case of the W distribution, the experimental data mostly lie in the middle between the NRQCD and CSM predictions, slightly favouring the former. We conclude from Figs. 3–7 that the H1 data [12] tends to support the NRQCD predictions, while, in general, it overshoots the CSM predictions. In Figs. 8 and 9, we present our NRQCD and CSM predictions for the $(p_T^*)^2$ and y distributions, respectively, although there are no experimental data to compare them with.

At this point, we should compare our numerical results for the cross section of $e + p \rightarrow e + J/\psi + j + X$ with the ones presented in Table II of Ref. [22]. To this end, we adopt the theoretical input and kinematic conditions from Ref. [22]. Specifically, the authors of Ref. [22] evaluated $\alpha_s^{(n_f)}(\mu)$ with $n_f = 4$ and $\Lambda^{(4)} = 130$ MeV, employed the LO proton PDF set by Glück, Reya, and Vogt [33], took the NRQCD MEs to be $\langle \mathcal{O}^\psi [^3S_1^{(1)}] \rangle = 1.1 \text{ GeV}^3$, $\langle \mathcal{O}^\psi [^1S_0^{(8)}] \rangle = 1 \times 10^{-2} \text{ GeV}^3$, $\langle \mathcal{O}^\psi [^3S_1^{(8)}] \rangle = 1.12 \times 10^{-2} \text{ GeV}^3$, and $\langle \mathcal{O}^\psi [^3P_0^{(8)}] \rangle / m_c^2 = 5 \times 10^{-3} \text{ GeV}^3$, and required that $30 < W < 150 \text{ GeV}$. All their other choices, except for the cuts on Q^2 , p_T , p_T^* , and z , coincide with our default settings. The outcome of this comparison is presented in Table 1. We are unable to determine the source of discrepancy.

Table 1: Comparison of our results for the CS and CO contributions to $\sigma(e + p \rightarrow e + J/\psi + j + X)$ in DIS with the ones of Ref. [22].

Type	Cuts	Ref. [22]	Our result
CS	$Q^2 > 4 \text{ GeV}^2$	89 pb	107 pb
CS	$Q^2, p_T^2 > 4 \text{ GeV}^2$	40 pb	62 pb
CS	$Q^2 > 4 \text{ GeV}^2, (p_T^*)^2 > 2 \text{ GeV}^2, z < 0.8$	13 pb	24 pb
CO	$Q^2 > 4 \text{ GeV}^2, (p_T^*)^2 > 2 \text{ GeV}^2, z < 0.8$	8 pb	16 pb

Before the advent of the NRQCD factorization formalism [1], one of the major moti-

vations to study J/ψ inclusive production in ep DIS was to extract the gluon PDF of the proton $f_{g/p}(x, M)$ [24,25]. In fact, to LO the CSM, the only contributing partonic subprocess is $e + g \rightarrow e + c\bar{c} [^3S_1^{(1)}] + g$, and $\langle \mathcal{O}^\psi [^3S_1^{(1)}] \rangle$ is well determined from the partial width of the J/ψ decay to lepton pairs. Furthermore, x is experimentally accessible through the relation $x = 1 - M_{X'}^2/[y(1-z)S]$, and $M = \sqrt{Q^2 + M_\psi^2}$ is a plausible choice. To LO in NRQCD, this task is somewhat impeded by the presence of CO partonic subprocesses with quarks or antiquarks in the initial state and by the presently still considerable uncertainties in the CO MEs. We observe from Figs. 3–7 that the CO contributions lead to a dramatic increase in cross section relative to the CSM predictions. In fact, if we consider the total cross section evaluated with the H1 acceptance cuts [12], then the CSM contribution only makes up 25% of the full NRQCD result. Thus, the present uncertainties in the CO MEs do constitute a serious problem. However, the quark- and antiquark-induced CO subprocesses only yield a minor contribution, less than 5% of the total cross section. Thus, J/ψ inclusive production in ep DIS remains to be a sensitive probe of the gluon PDF of the proton if we pass from the CSM to NRQCD.

4 Conclusions

We provided, in analytic form, the cross sections of the partonic subprocesses $e + a \rightarrow e + c\bar{c}[n] + a$, where $a = g, q, \bar{q}$ and $n = ^3S_1^{(1)}, ^1S_0^{(8)}, ^3S_1^{(8)}, ^3P_J^{(8)}$, to LO in the NRQCD factorization formalism [1]. Using these results, we then studied the cross section of $e + p \rightarrow e + J/\psi + j + X$ in DIS under HERA kinematic conditions and compared various of its distributions with recent H1 data [12], from which the contribution of elastic J/ψ production was separated by a suitable acceptance cut on z . It turned out that, in general, the experimental data agrees reasonably well with our NRQCD predictions, while they tend to disfavour the CSM ones. However, a familiar feature of J/ψ inclusive photoproduction in ep scattering at HERA [15,16] carries over to DIS, namely that the cross section predicted to LO in NRQCD exhibits a distinct rise as $z \rightarrow 1$, which is absent in the experimental z distribution.

At this point, it is still premature to jump to conclusions concerning the experimental verification or falsification of the NRQCD factorization hypothesis. On the one hand, the theoretical predictions for J/ψ inclusive production in $p\bar{p}$ scattering at the Tevatron [3,5] and in ep DIS at HERA are of LO in α_s and v , and they suffer from considerable uncertainties, mostly from the scale dependences and from the lack of information on the CO MEs. On the other hand, the experimental errors are still rather sizeable [6,12,13]. The latter will be dramatically reduced with the upgrades of HERA and the Tevatron, and with the advent of CERN LHC and hopefully a future e^+e^- linear collider such as DESY TESLA. On the theoretical side, it is necessary to calculate the NLO corrections to the hard-scattering cross sections and to include the effective operators which are suppressed by higher powers of v .

Acknowledgements

We acknowledge the collaboration of Jungil Lee at the initial stage of this work. We thank Jochen Bartels for instructive comments on the possibilities of suppressing the contribution from J/ψ diffractive production in ep DIS. We are grateful to Sean Fleming for helpful communications concerning Ref. [22]. We are indepted to Arnd Meyer, Susanne Mohrdieck, and Beate Naroska for numerous useful discussions regarding Ref. [12,13,14]. The work of L.Z. was supported by the Studienstiftung des deutschen Volkes through a PhD scholarship. This work was supported in part by the Deutsche Forschungsgemeinschaft through Grant No. KN 365/1-1, by the Bundesministerium für Bildung und Forschung through Grant No. 05 HT1GUA/4, by the European Commission through the Research Training Network *Quantum Chromodynamics and the Deep Structure of Elementary Particles* under Contract No. ERBFMRX-CT98-0194, and by Sun Microsystems through Academic Equipment Grant No. EDUD-7832-000332-GER.

A Partonic cross sections

In this Appendix, we present analytic expressions for the coefficients $F_a[n]$, $T_a[n]$, and $L_a[n]$ appearing in Eq. (13). In order to compactify the expressions, it is useful to introduce the Lorentz invariants $s = 2q \cdot p$, $t = -2p \cdot p'$, and $u = -2q \cdot p'$, which are related to the partonic Mandelstam variables by $s = \hat{s} + Q^2$, $t = \hat{t}$, and $u = \hat{u} + Q^2$, respectively. In the following, e_q is the fractional electric charge of quark q .

$$e + q(\bar{q}) \rightarrow c\bar{c} \left[{}^3S_1^{(1)} \right] + q(\bar{q}): \quad F = T = L = 0. \quad (\text{A.1})$$

$$e + q(\bar{q}) \rightarrow c\bar{c} \left[{}^1S_0^{(8)} \right] + q(\bar{q}):$$

$$F = \frac{-16\pi^2 e_c^2 \alpha_s^2}{3M_\psi s^4 t (s+u)^2},$$

$$T = 2Q^4 t^2 + 2Q^2 st(s+u) + s^2(s^2 + u^2),$$

$$L = -2t(Q^2 t + su). \quad (\text{A.2})$$

$$e + q(\bar{q}) \rightarrow c\bar{c} \left[{}^3S_1^{(8)} \right] + q(\bar{q}):$$

$$F = \frac{-8\pi^2 e_q^2 \alpha_s^2}{9M_\psi^3 s^4 (Q^2 - s)^2 (Q^2 - u)^2},$$

$$T = 2Q^6 t^2 (2s+t) + 2Q^4 s[s^2 u - st(3t-2u) - 2t^3] + Q^2 s^2[s^2(t-2u) + 2s(t^2 - 4tu - u^2) + t(2t^2 - 2tu - u^2)] + s^3 u(s^2 + 2st + 2t^2 + 2tu + u^2),$$

$$L = -2(Q^2 - s)^2 t(s+t)^2. \quad (\text{A.3})$$

$$e + q(\bar{q}) \rightarrow c\bar{c} \left[{}^3P_J^{(8)} \right] + q(\bar{q}):$$

$$F = \frac{64\pi^2 e_c^2 \alpha_s^2}{3M_\psi^3 s^4 t (s+u)^4},$$

$$\begin{aligned}
T &= 8Q^6t[2s^2 + st + t(2t + u)] - 2Q^4[4s^4 + 12s^3t + s^2(19t^2 + 8tu + 4u^2) + 2st(6t^2 \\
&\quad + tu - 2u^2) + t^2(8t^2 + 12tu + 7u^2)] + 2Q^2s[6s^4 + s^3(7t + 6u) + s^2(4t^2 + 3tu \\
&\quad + 6u^2) - su(8t^2 + 3tu - 6u^2) - tu(8t^2 + 12tu + 7u^2)] - s^2(s + u)[7s^3 + s^2(12t \\
&\quad + 7u) + s(8t^2 + 16tu + 7u^2) + u(8t^2 + 12tu + 7u^2)], \\
L &= 8Q^4t[s^2 - st - t(2t + u)] - 2Q^2[2s^4 + 4s^3t + s^2(5t^2 + 8tu + 2u^2) - 2st(6t^2 \\
&\quad + tu - 2u^2) - t^2(8t^2 + 12tu + 7u^2)] + 2s(s + u)[2s^3 + 2s^2t + s(8t^2 + 5tu \\
&\quad + 2u^2) + t(8t^2 + 12tu + 7u^2)]. \tag{A.4}
\end{aligned}$$

$$e + g \rightarrow c\bar{c} \left[{}^3S_1^{(1)} \right] + g:$$

$$\begin{aligned}
F &= \frac{64\pi^2 e_c^2 \alpha \alpha_s^2}{27M_\psi s^4 (s+t)^2 (s+u)^2 (t+u)^2}, \\
T &= -4Q^6 t^2 (s^2 + t^2) + 2Q^4 t [s^3 (3t - 2u) + 3s^2 t (t + u) + 2st^2 (t - u) + 2t^3 (t + u)] \\
&\quad - 2Q^2 s [s^3 (t - u)^2 - 2s^2 tu (t + u) - st^2 u (2t - u) - 2t^3 u (t + u)] + 2s^2 [s^3 (t^2 \\
&\quad + tu + u^2) + s^2 (t + u)^3 + stu (t^2 + 3tu + u^2) + t^2 u^2 (t + u)], \\
L &= -2Q^4 t^2 (s^2 - 2t^2) + 2Q^2 t (s^2 - 2t^2) [s(t - u) + t(t + u)] - s [s^3 (t^2 + u^2) \\
&\quad + 2s^2 t^2 (t + u) + st^2 (t^2 + 6tu + u^2) + 4t^3 u (t + u)]. \tag{A.5}
\end{aligned}$$

$$e + g \rightarrow c\bar{c} \left[{}^1S_0^{(8)} \right] + g:$$

$$\begin{aligned}
F &= \frac{24\pi^2 e_c^2 \alpha \alpha_s^2}{M_\psi s^4 t (s+t)^2 (s+u)^2 (t+u)^2}, \\
T &= 2Q^6 t^3 u^2 + 2Q^4 st^2 u [s(t + u) + t^2 + tu + 2u^2] + Q^2 s^2 t [s^4 + 2s^3 (t + u) \\
&\quad + 3s^2 (t + u)^2 + 2s(t^3 + 3t^2 u + 4tu^2 + 2u^3) + t^4 + 2t^3 u + 5t^2 u^2 + 4tu^3 + 3u^4] \\
&\quad + s^3 u [s^4 + 2s^3 (t + u) + 3s^2 (t + u)^2 + 2s(t + u)^3 + (t^2 + tu + u^2)^2], \\
L &= -2Q^4 t^3 u^2 - 2Q^2 st^2 u [s(t + u) + t^2 + tu + 2u^2] - s^2 t [s^2 (t + u)^2 \\
&\quad + 2s(t^3 + 2t^2 u + 2tu^2 + u^3) + t^4 + 2t^3 u + 3t^2 u^2 + 2tu^3 + 2u^4]. \tag{A.6}
\end{aligned}$$

$$e + g \rightarrow c\bar{c} \left[{}^3S_1^{(8)} \right] + g:$$

$$\begin{aligned}
F &= \frac{15}{8} F \left(e + g \rightarrow c\bar{c} \left[{}^3S_1^{(1)} \right] + g \right), \\
T &= T \left(e + g \rightarrow c\bar{c} \left[{}^3S_1^{(1)} \right] + g \right), \\
L &= L \left(e + g \rightarrow c\bar{c} \left[{}^3S_1^{(1)} \right] + g \right). \tag{A.7}
\end{aligned}$$

$$e + g \rightarrow c\bar{c} \left[{}^3P_J^{(8)} \right] + g:$$

$$\begin{aligned}
F &= \frac{96\pi^2 e_c^2 \alpha \alpha_s^2}{M_\psi^3 s^4 t (s+t)^3 (s+u)^4 (t+u)^3}, \\
T &= -8Q^8 t^2 [2s^5 t - 2s^4 u^2 + s^3 t^2 (2t - 3u) - s^2 tu (t^2 + 3tu - 3u^2) - stu (2t^3 + t^2 u - tu^2)
\end{aligned}$$

$$\begin{aligned}
& -u^3) + t^2u^3(2t+u)] + 2Q^6t[4s^7(t+u) + 4s^6(5t^2+2u^2) + 4s^5(5t^3+6t^2u-2tu^2 \\
& + 4u^3) + 2s^4(9t^4-9t^3u+4t^2u^2-6tu^3+4u^4) + s^3(12t^5-2t^4u-29t^3u^2+33t^2u^3 \\
& - 12tu^4+4u^5) - s^2t(2t^5+20t^4u+25t^3u^2-t^2u^3-16tu^4+4u^5) - st^2u(12t^4+26t^3u \\
& + 2t^2u^2+tu^3+u^4) - t^3u^2(2t^3-6t^2u-15tu^2-7u^3)] - 2Q^4[2s^8(3t^2+tu-2u^2) \\
& + s^7(21t^3+3t^2u+10tu^2-8u^3) + s^6(28t^4+15t^3u-15t^2u^2+22tu^3-12u^4) + s^5(27t^5 \\
& + 11t^4u+8t^3u^2-20t^2u^3+26tu^4-8u^5) + s^4(16t^6+17t^5u-20t^4u^2+2t^3u^3-33t^2u^4 \\
& + 18tu^5-4u^6) + s^3t(2t^6+8t^5u-3t^4u^2-19t^3u^3-19t^2u^4-17tu^5+6u^6) - s^2t^2(2t^6 \\
& + 14t^5u+30t^4u^2+33t^3u^3+46t^2u^4+21tu^5+4u^6) - 2st^3u(2t^5+10t^4u+16t^3u^2 \\
& + 20t^2u^3+19tu^4+7u^5) - 2t^6u^2(t+u)^2] + Q^2s[s^8(7t^2-5tu-12u^2) + s^7(25t^3+3t^2u \\
& - 18tu^2-36u^3) + s^6(37t^4+25t^3u-12t^2u^2-20tu^3-60u^4) + s^5(39t^5+39t^4u+16t^3u^2 \\
& - 18t^2u^3-6tu^4-60u^5) + s^4(29t^6+83t^5u+72t^4u^2+88t^3u^3+40t^2u^4+22tu^5-36u^6) \\
& + s^3(9t^7+75t^6u+148t^5u^2+176t^4u^3+178t^3u^4+102t^2u^5+22tu^6-12u^7) + s^2tu(22t^6 \\
& + 107t^5u+199t^4u^2+211t^3u^3+177t^2u^4+73tu^5+9u^6) + st^2u^2(17t^5+69t^4u+107t^3u^2 \\
& + 105t^2u^3+71tu^4+21u^5) + 4t^5u^3(t+u)^2] + s^2(s+u)[7s^7u(t+u) + s^6u(25t^2+38tu \\
& + 21u^2) + s^5(2t^4+47t^3u+88t^2u^2+78tu^3+35u^4) + s^4(4t^5+63t^4u+132t^3u^2 \\
& + 156t^2u^3+98tu^4+35u^5) + s^3(2t^6+47t^5u+136t^4u^2+190t^3u^3+156t^2u^4+78tu^5 \\
& + 21u^6) + s^2u(13t^6+70t^5u+136t^4u^2+132t^3u^3+88t^2u^4+38tu^5+7u^6) + stu^2(13t^5 \\
& + 47t^4u+63t^3u^2+47t^2u^3+25tu^4+7u^5) + 2t^4u^3(t+u)^2], \\
L = & -8Q^6t^2[s^5t-s^4u^2-2s^3t^3+s^2t^2u(t+3u)+stu(2t^3+t^2u-tu^2-u^3)-t^2u^3(2t+u)] \\
& + 2Q^4t[2s^7(t+u) + 4s^6(2t^2+u^2) - s^5(t^3-t^2u+2tu^2-8u^3) - s^4(21t^4+13t^3u \\
& + 18t^2u^2-2tu^3-4u^4) - 2s^3(6t^5+10t^4u+t^3u^2+4t^2u^3-6tu^4-u^5) + 2s^2t(t^5+10t^4u \\
& + 11t^3u^2+9t^2u^3+6tu^4+5u^5) + st^2u(12t^4+26t^3u+2t^2u^2+tu^3+u^4) + t^3u^2(2t^3 \\
& - 6t^2u-15tu^2-7u^3)] - 4Q^2[s^8(t^2-u^2) + s^7(3t^3+tu^2-2u^3) - s^6(2t^4+2t^3u+2t^2u^2 \\
& - tu^3+3u^4) - s^5(12t^5+16t^4u+16t^3u^2-t^2u^3+tu^4+2u^5) - s^4(10t^6+28t^5u+28t^4u^2 \\
& + 13t^3u^3-7t^2u^4+3tu^5+u^6) - s^3t(t^6+9t^5u+18t^4u^2+t^3u^3-15t^2u^4-10tu^5+2u^6) \\
& + s^2t^2(t^6+7t^5u+13t^4u^2+18t^3u^3+35t^2u^4+24tu^5+6u^6) + st^3u(2t^5+10t^4u+16t^3u^2 \\
& + 20t^2u^3+19tu^4+7u^5) + t^6u^2(t+u)^2] - 2s(s+u)[2s^7u(t+u) + 2s^6u(3t^2+3tu \\
& + 2u^2) + s^5(5t^4+15t^3u+18t^2u^2+14tu^3+6u^4) + s^4(15t^5+38t^4u+53t^3u^2+40t^2u^3 \\
& + 22tu^4+4u^5) + s^3(15t^6+52t^5u+88t^4u^2+81t^3u^3+47t^2u^4+19tu^5+2u^6) + s^2t(5t^6 \\
& + 32t^5u+78t^4u^2+90t^3u^3+68t^2u^4+34tu^5+9u^6) + st^2u(7t^5+31t^4u+47t^3u^2+39t^2u^3 \\
& + 23tu^4+7u^5) + 2t^5u^2(t+u)^2]. \tag{A.8}
\end{aligned}$$

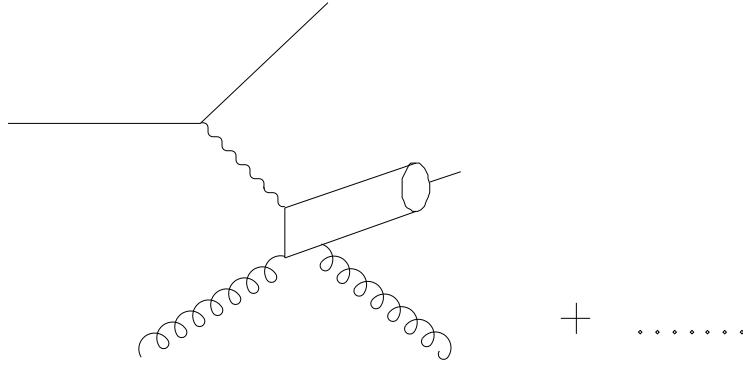
References

- [1] G.T. Bodwin, E. Braaten, G.P. Lepage, Phys. Rev. D 51 (1995) 1125;
G.T. Bodwin, E. Braaten, G.P. Lepage, Phys. Rev. D 55 (1997) 5853, Erratum.

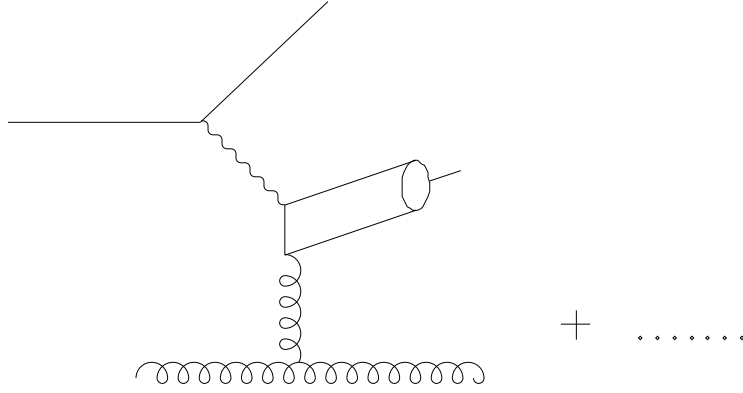
- [2] E.L. Berger, D. Jones, Phys. Rev. D 23 (1981) 1521.
- [3] R. Baier, R. Rückl, Phys. Lett. 102 B (1981) 364;
R. Baier, R. Rückl, Z. Phys. C 19 (1983) 251;
B. Humpert, Phys. Lett. B 184 (1987) 105;
R. Gastmans, W. Troost, T.T. Wu, Phys. Lett. B 184 (1987) 257;
R. Gastmans, W. Troost, T.T. Wu, Nucl. Phys. B 291 (1987) 731.
- [4] E. Braaten, S. Fleming, Phys. Rev. Lett. 74 (1995) 3327;
E. Braaten, T.C. Yuan, Phys. Rev. D 52 (1995) 6627.
- [5] P. Cho, A.K. Leibovich, Phys. Rev. D 53 (1996) 150;
P. Cho, A.K. Leibovich, Phys. Rev. 53 (1996) 6203.
- [6] CDF Collaboration, F. Abe et al., Phys. Rev. Lett. 69 (1992) 3704;
CDF Collaboration, F. Abe et al., Phys. Rev. Lett. 71 (1993) 2537;
CDF Collaboration, F. Abe et al., Phys. Rev. Lett. 79 (1997) 572;
CDF Collaboration, F. Abe et al., Phys. Rev. Lett. 79 (1997) 578;
D0 Collaboration, S. Abachi et al., Phys. Lett. B 370 (1996) 239;
D0 Collaboration, B. Abbott et al., Phys. Rev. Lett. 82 (1999) 35.
- [7] E. Braaten, S. Fleming, T.C. Yuan, Ann. Rev. Nucl. Part. Sci. 46 (1996) 197;
B.A. Kniehl, G. Kramer, Phys. Lett. B 413 (1997) 416;
M. Krämer, Prog. Part. Nucl. Phys. 47 (2001) 141.
- [8] M. Beneke, M. Krämer, Phys. Rev. D 55 (1997) 5269;
A.K. Leibovich, Phys. Rev. D 56 (1997) 4412;
B.A. Kniehl, J. Lee, Phys. Rev. D 62 (2000) 114027;
S. Fleming, A.K. Leibovich, I.Z. Rothstein, Phys. Rev. D 64 (2001) 036002.
- [9] M. Beneke, M. Krämer, M. Vanttinen, Phys. Rev. D 57 (1998) 4258.
- [10] E. Braaten, B.A. Kniehl, J. Lee, Phys. Rev. D 62 (2000) 094005.
- [11] S.J. Brodsky, L. Frankfurt, J.F. Gunion, A.H. Mueller, M. Strikman, Phys. Rev. D 50 (1994) 3134.
- [12] A. Meyer, PhD Thesis, Universität Hamburg, 1998, Report No. DESY-THESIS-1998-012;
A. Meyer, private communication;
S. Mohrdeieck, private communication.
- [13] H1 Collaboration, C. Adloff et al., Eur. Phys. J. C 10 (1999) 373;
B. Naroska, on behalf of the H1 and ZEUS Collaborations, in: S. Söldner-Rembold (Ed.), Photon 99: Proceedings of the International Conference on the Structure and Interactions of the Photon, including the 12th International Workshop on Photon-Photon Collisions, Freiburg, Germany, 23–27 May 1999, Nucl. Phys. B (Proc. Suppl.)

- 82 (2000) 187;
 B. Naroska, on behalf of the H1 and ZEUS Collaborations, in: G. Grindhammer, B.A. Kniehl, G. Kramer, W. Ochs (Eds.), Proceedings of the Ringberg Workshop on New Trends in HERA Physics 2001, Tegernsee, Germany, 17–22 June 2001, J. Phys. G (to appear);
 A. Bertolin, on behalf of the H1 and ZEUS Collaborations, in: K. Huitu, H. Kurki-Suonio, J. Maalampi (Eds.), High Energy Physics 99: Proceedings of the International Europhysics Conference on High Energy Physics, Tampere, Finland, 15–21 July 1999, Institute of Physics Publishing, Bristol and Philadelphia, 2000, p. 580.
- [14] S. Mohrdieck, PhD Thesis, Universität Hamburg, 2000, Report No. DESY-THESIS-2000-059.
 - [15] M. Cacciari, M. Krämer, Phys. Rev. Lett. 76 (1996) 4128.
 - [16] P. Ko, J. Lee, H.S. Song, Phys. Rev. D 54 (1996) 4312;
 P. Ko, J. Lee, H.S. Song, Phys. Rev. D 60 (1999) 119902, Erratum.
 - [17] H1 Collaboration, S. Aid et al., Nucl. Phys. B 472 (1996) 3.
 - [18] ZEUS Collaboration, J. Breitweg et al., Z. Phys. C 76 (1997) 599.
 - [19] B. Cano-Coloma, M.A. Sanchis-Lozano, Phys. Lett. B 406 (1997) 232;
 B. Cano-Coloma, M.A. Sanchis-Lozano, Nucl. Phys. B 508 (1997) 753;
 B.A. Kniehl, G. Kramer, Z. Phys. C 6 (1999) 493.
 - [20] M. Beneke, I.Z. Rothstein, M.B. Wise, Phys. Lett. B 408 (1997) 373.
 - [21] K. Sridhar, A.D. Martin, W.J. Stirling, Phys. Lett. B 438 (1998) 211;
 Ph. Hägler, R. Kirschner, A. Schäfer, L. Szymanowski, O.V. Teryaev, Phys. Rev. D 63 (2001) 077501.
 - [22] S. Fleming, T. Mehen, Phys. Rev. D 57 (1998) 1846;
 S. Fleming, private communication.
 - [23] J.G. Körner, J. Cleymans, M. Kuroda, G.J. Gounaris, Phys. Lett. 114B (1982) 195.
 - [24] J.-Ph. Guillet, Z. Phys. C 39 (1988) 75.
 - [25] H. Merabet, J.F. Mathiot, R. Mendez-Galain, Z. Phys. C 62 (1994) 639.
 - [26] D. Krücker, PhD Thesis, RWTH Aachen, 1995.
 - [27] F. Yuan, K.-T. Chao, Phys. Rev. D 63 (2001) 034017.
 - [28] Particle Data Group, D.E. Groom et al., Eur. Phys. J. C 15 (2000) 1.
 - [29] D. Graudenz, Phys. Rev. D 49 (1994) 3291.

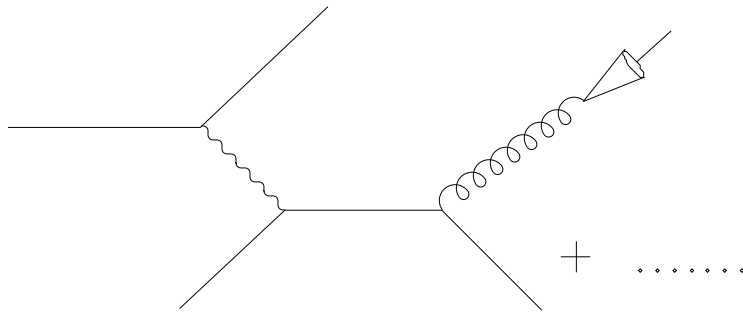
- [30] A. Petrelli, M. Cacciari, M. Greco, F. Maltoni, M.L. Mangano, Nucl. Phys. B 514 (1998) 245;
F. Maltoni, M.L. Mangano, A. Petrelli, Nucl. Phys. B 519 (1998) 361.
- [31] A.D. Martin, R.G. Roberts, W.J. Stirling, R.S. Thorne, Eur. Phys. J. C 4 (1998) 463.
- [32] CTEQ Collaboration, H.L. Lai et al., Eur. Phys. J. C 12 (2000) 375.
- [33] M. Glück, E. Reya, A. Vogt, Z. Phys. C 67 (1995) 433.



(a)



(b)



(c)

Figure 1: Representative Feynman diagrams for the partonic subprocesses $e + a \rightarrow e + c\bar{c}[n] + a$, where $a = g, q, \bar{q}$ and $n = {}^3S_1^{(1)}, {}^1S_0^{(8)}, {}^3S_1^{(8)}, {}^3P_J^{(8)}$. There are six diagrams of the type shown in part (a), two ones of the type shown in part (b), and two ones of the type shown in part (c). There are two more diagrams that are obtained from the diagrams of the type shown in part (b) by replacing the external gluon lines with quark ones. The CS process only proceeds through the diagrams shown in part (a).

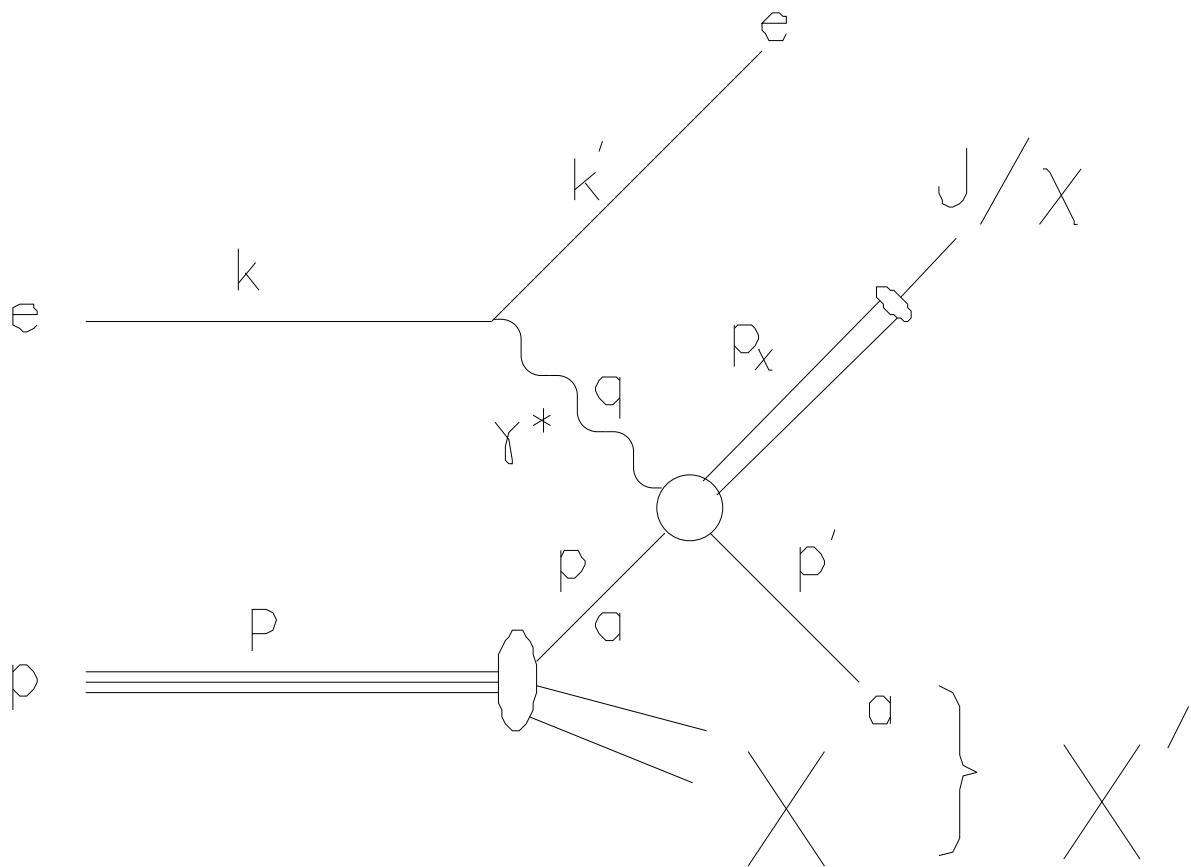


Figure 2: Schematic representation of $e + p \rightarrow e + J/\psi + j + X$ explaining the four-momentum assignments.

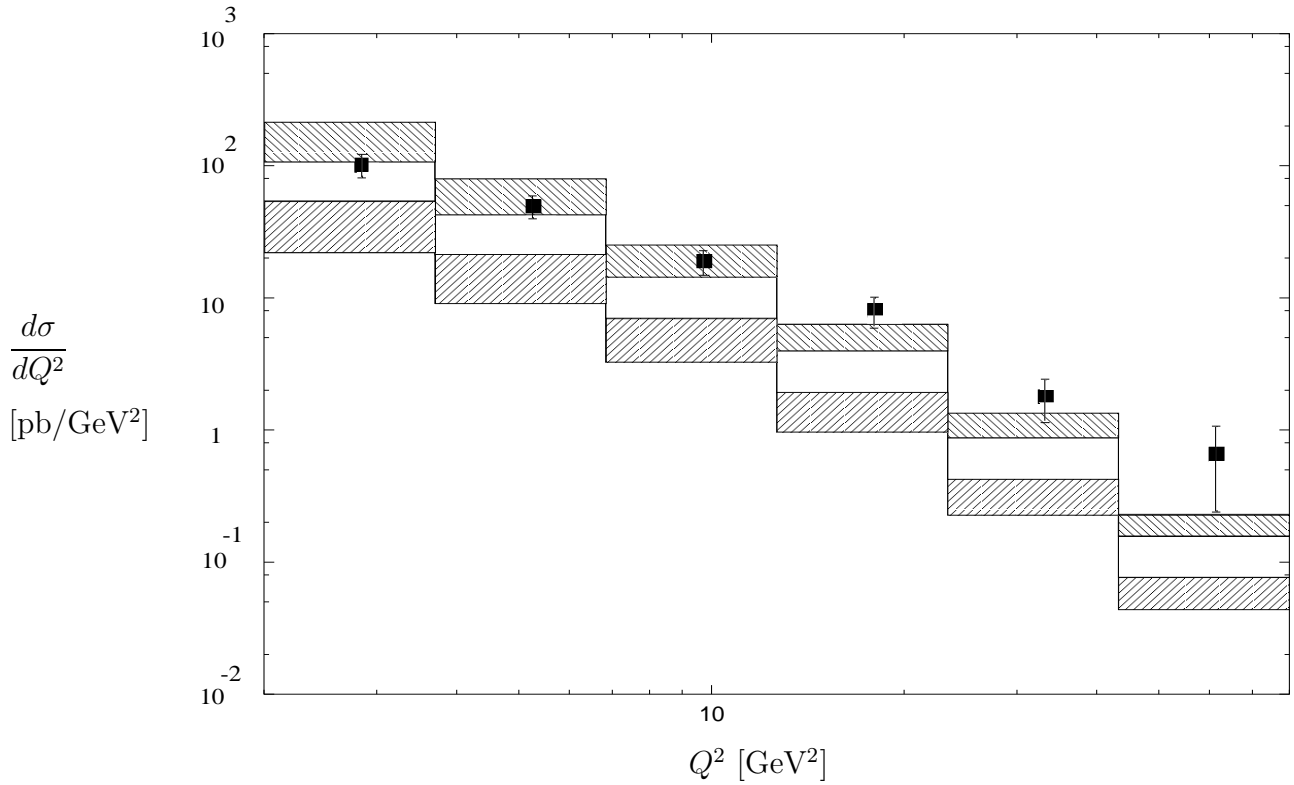


Figure 3: The Q^2 distribution of J/ψ inclusive production in ep DIS measured with the H1 detector [12] is compared with the LO NRQCD (upper histogram) and CSM (lower histogram) predictions.

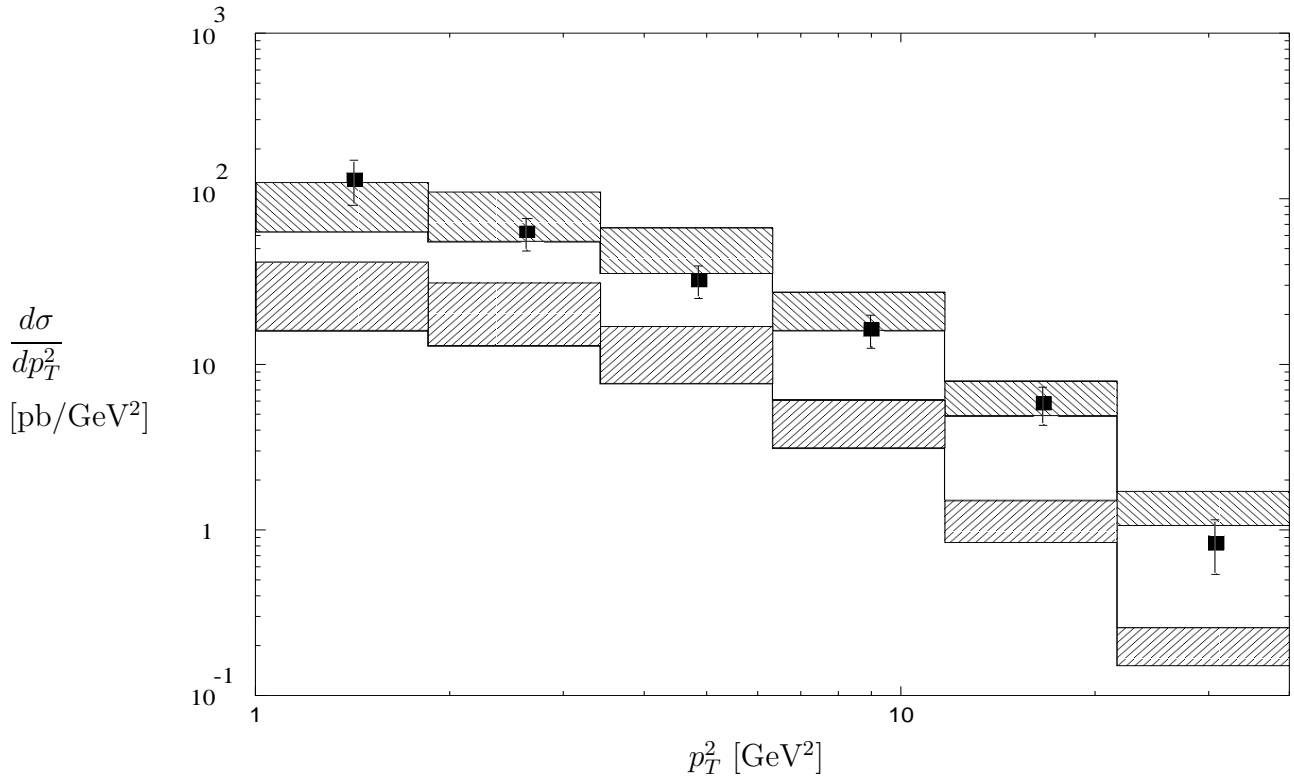


Figure 4: The p_T^2 distribution of J/ψ inclusive production in ep DIS measured with the H1 detector [12] is compared with the LO NRQCD (upper histogram) and CSM (lower histogram) predictions.

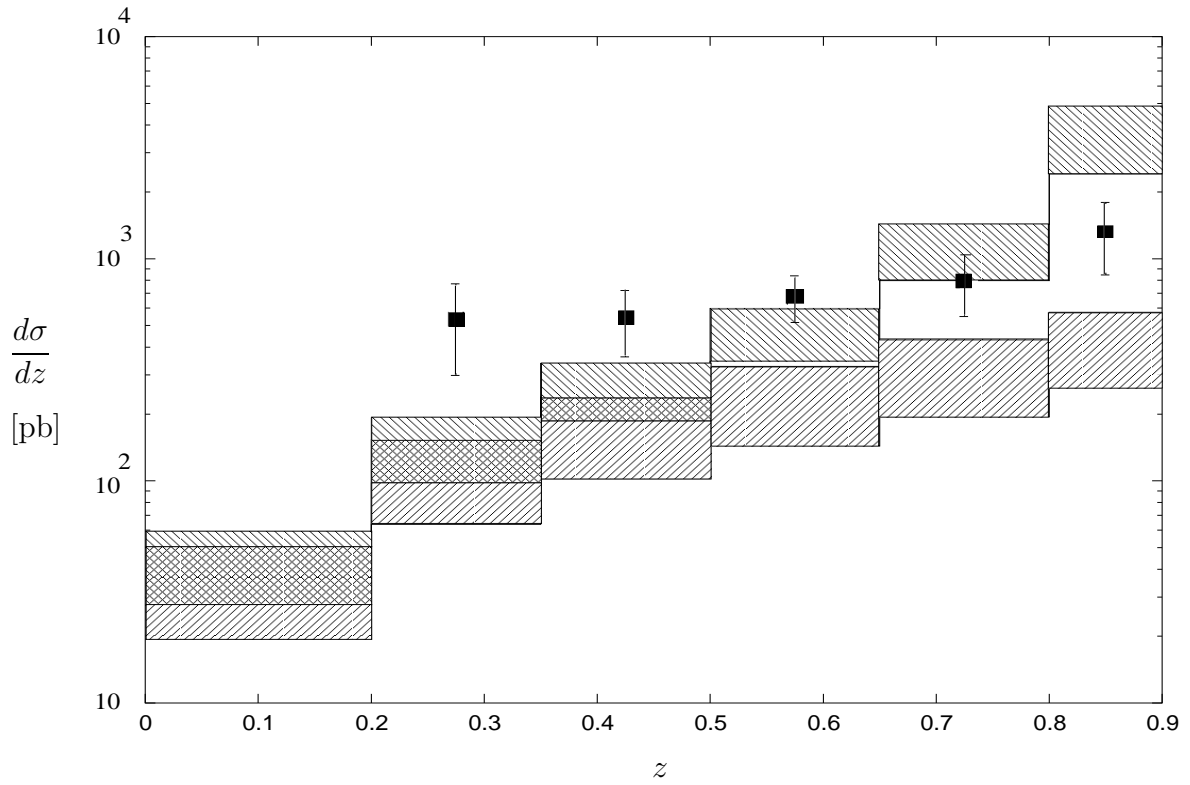


Figure 5: The z distribution of J/ψ inclusive production in ep DIS measured with the H1 detector [12] is compared with the LO NRQCD (upper histogram) and CSM (lower histogram) predictions.

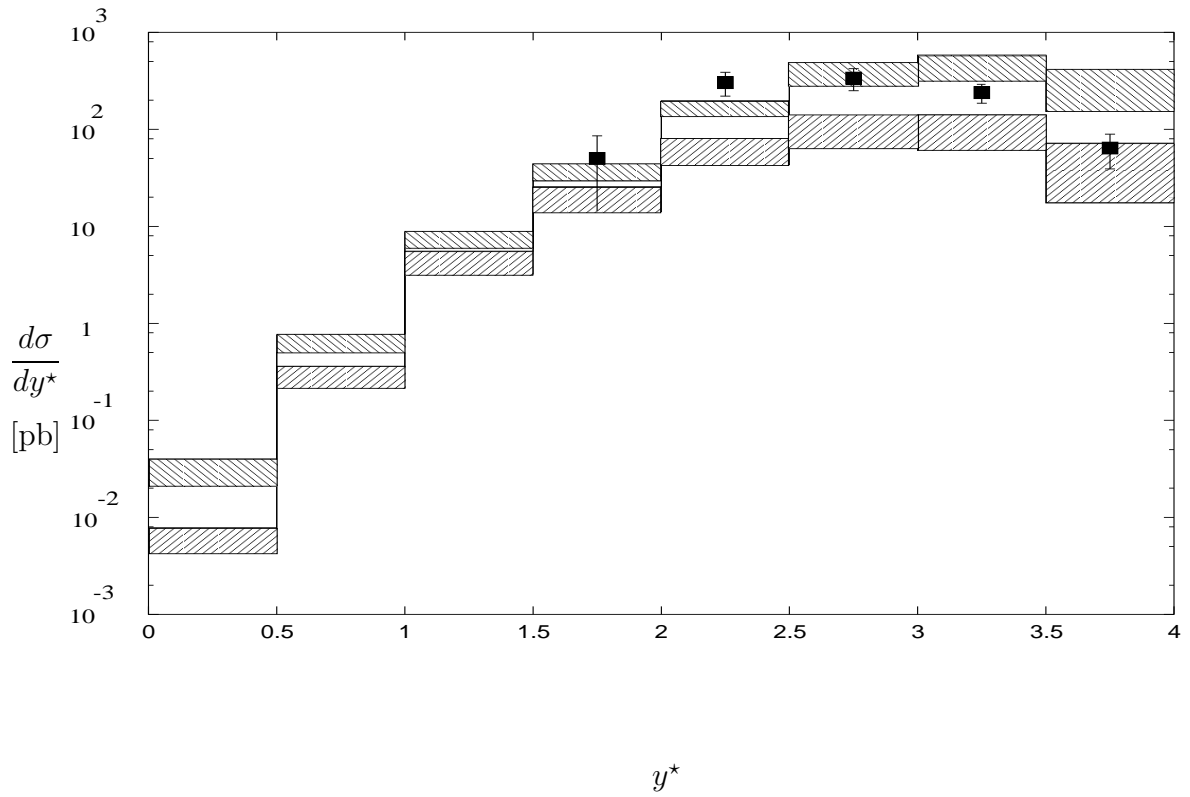


Figure 6: The y^* distribution of J/ψ inclusive production in ep DIS measured with the H1 detector [12] is compared with the LO NRQCD (upper histogram) and CSM (lower histogram) predictions.

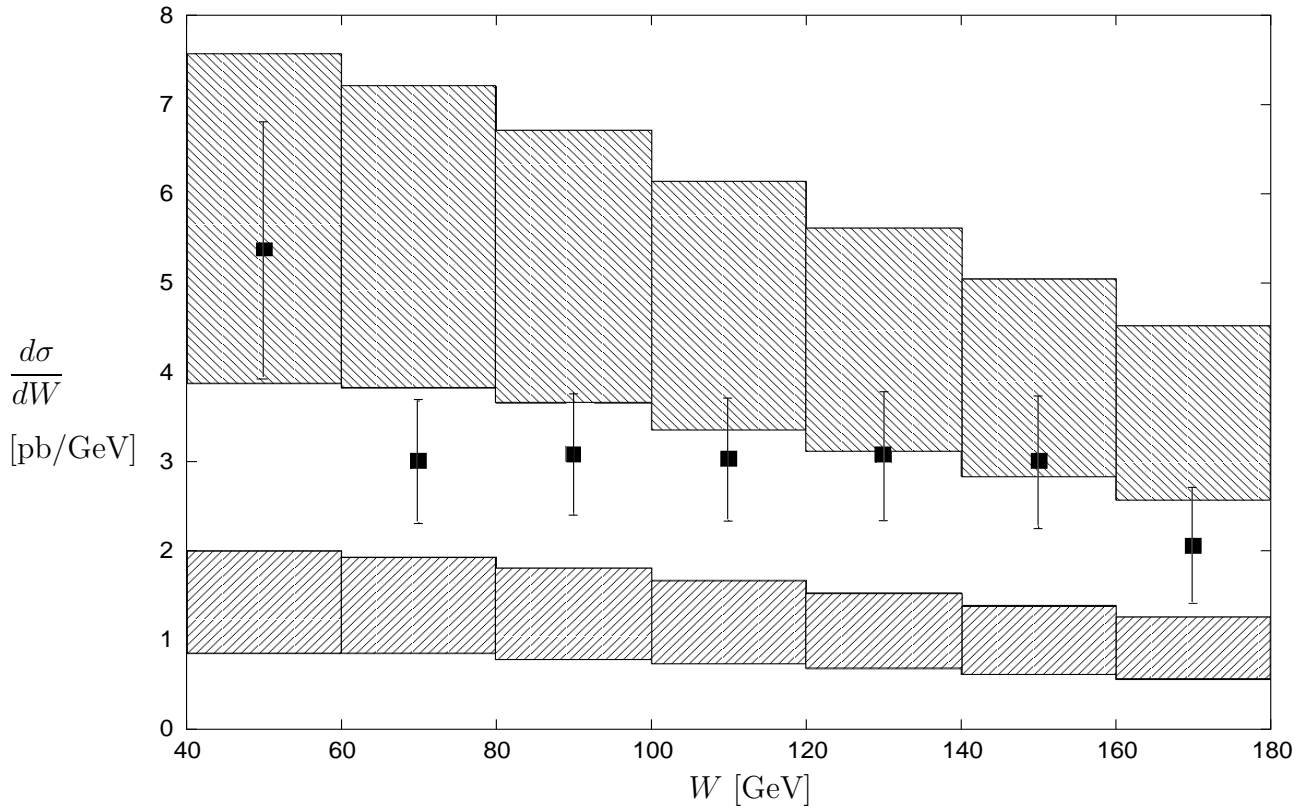


Figure 7: The W distribution of J/ψ inclusive production in ep DIS measured with the H1 detector [12] is compared with the LO NRQCD (upper histogram) and CSM (lower histogram) predictions.

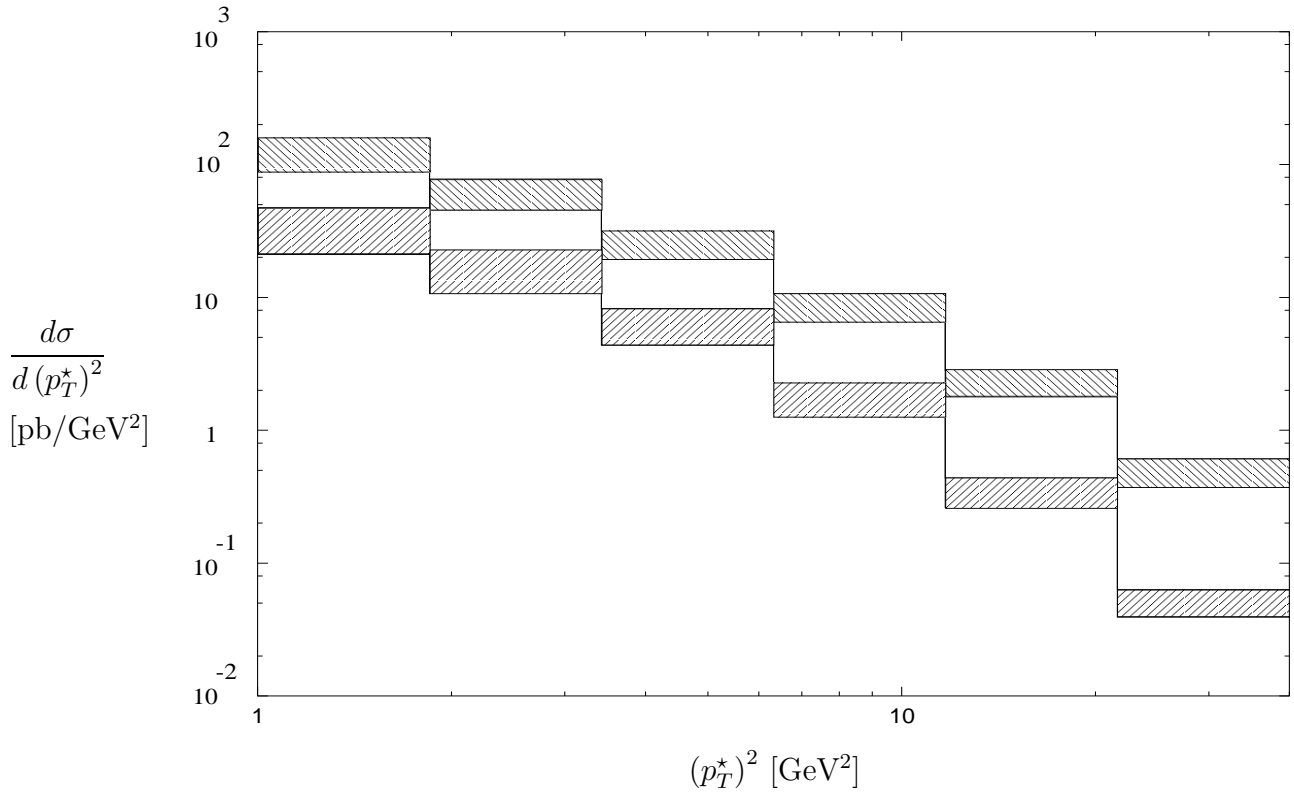


Figure 8: LO NRQCD (upper histogram) and CSM (lower histogram) predictions for the $(p_T^*)^2$ distribution of J/ψ inclusive production in ep DIS.

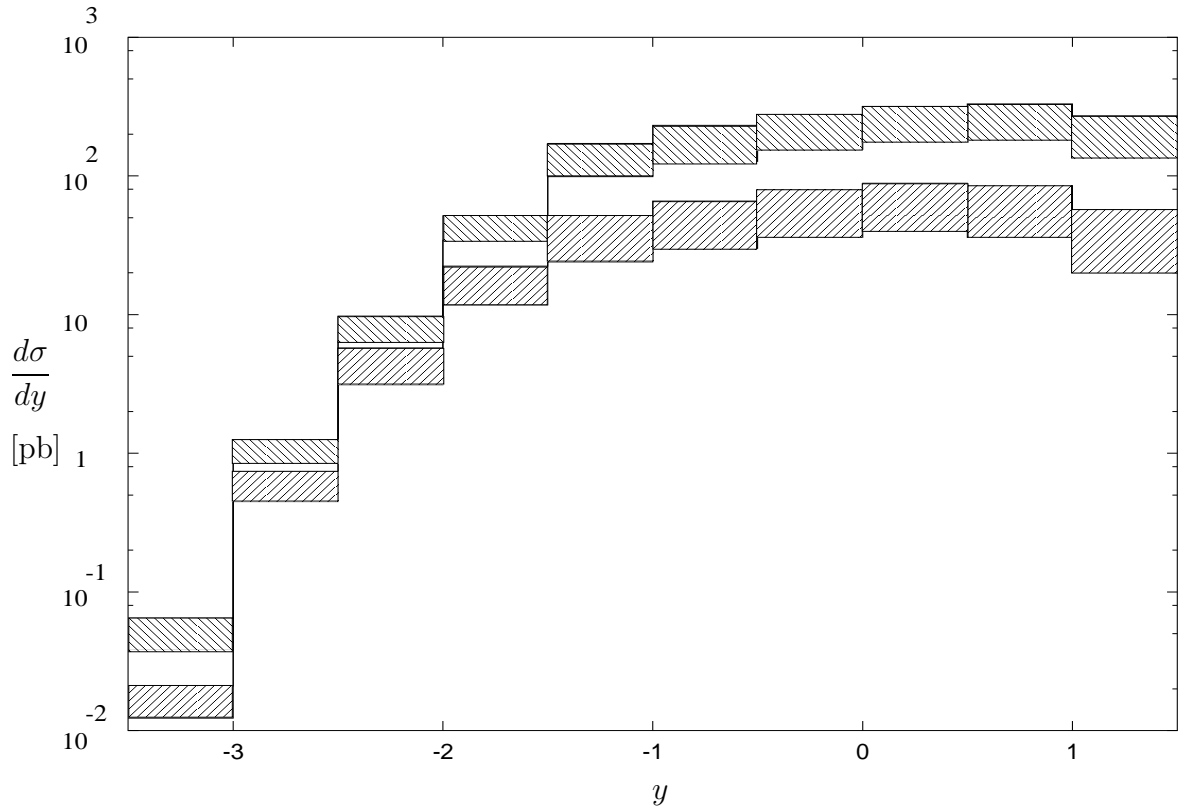


Figure 9: LO NRQCD (upper histogram) and CSM (lower histogram) predictions for the y distribution of J/ψ inclusive production in ep DIS.